journal

J. Am. Ceram. Soc., 91 [4] 1273–1280 (2008)
DOI: 10.1111/j.1551-2916.2008.02290.x

Microstructural Development of the AlN/Ti Diffusion Couple Annealed at 1000°C

Chia-Hsiang Chiu and Chien-Cheng Lin*,†

Department of Materials Science and Engineering, National Chiao Tung University, Hsinchu 30050, Taiwan

The microstructural development of an AlN/Ti diffusion couple, annealed at 1000°C in an argon atmosphere for 0.1–36 h, was investigated using analytical scanning electron microscopy and transmission electron microscopy. The decomposition and diffusion of Al and N atoms into Ti gave rise to various reaction layers at the interface. A δ-TiN layer was initially formed in the reaction zone between AlN and Ti, and the α_2-Ti_3Al layer subsequently developed between δ-TiN and Ti. Then an intergranular τ_1-Ti_3AlN phase was formed in the δ-TiN layer with the orientation relationships $[111]_{\tau_1\text{-}Ti_3AlN}//[111]_{\delta\text{-}TiN}$ and $(1\bar{1}0)_{\tau_1\text{-}Ti_3AlN}//(1\bar{1}0)_{\delta\text{-}TiN}$. The further diffusion of N atoms into the α_2-Ti_3Al layer led to the growth of δ-TiN and a twinned α_2-$Ti_3Al(N)$ solid solution, wherein N atoms went to one of the octahedral interstitial sites in an orderly manner upon cooling, resulting in the formation of τ_1-Ti_3AlN. The orientation relationships between τ_1-Ti_3AlN and α_2-$Ti_3Al(N)$ were $[111]_{\tau_1\text{-}Ti_3AlN}//[0001]_{\alpha_2\text{-}Ti_3Al(N)}$ and $(0\bar{1}1)_{\tau_1\text{-}Ti_3AlN}//(\bar{1}\bar{1}20)_{\alpha_2\text{-}Ti_3Al(N)}$. Finally, diffusion paths are proposed for the interfacial reactions at various stages.

I. Introduction

A low dielectric constant and good thermal dissipation are the two most important requirements for electronic packaging materials, because small modern VLSIs are operated at high power and high speed. AlN has been used as a replacement for alumina in electron packaging applications because it can fulfill these requirements.[1–3] Highly reactive Ti has been used as an interlayer because of good wetting and adhesion between Cu and AlN, while retaining a ductile layer to minimize residual stresses that are caused by the difference in thermal expansion coefficients.[4–6]

The reaction mechanisms and products at the AlN/Ti interface mentioned previously were inconsistent or conflicting because of variations in reactant types, annealing conditions, and methods of analysis. Table I summarizes some experimental results on the AlN/Ti interfaces.[6–16] As was noted, previous investigations were focused on the reaction of AlN with Ti thin film or foil.[6,8,11,12] Pinkas *et al.*[8] demonstrated that $TiAl_3$, ε-Ti_2N, α_2-Ti_3Al, and α-Ti(Al) solid solutions were formed in sequence at the Ti(film)/AlN interface after annealing at 600°C for 1–10 h. Imanaka and Notis[6] noted that τ_2-Ti_2AlN was formed at the Ti(film)/AlN interface after annealing at 800°–950°C. El-Sayed *et al.*[11] found δ-TiN, τ_1-Ti_3AlN, and α_2-Ti_3Al at the Ti(foil)/AlN interface after annealing at 1050°–1200°C for 2–20 h in a vacuum. After annealing at 1200°C for 11 h, the Ti foil (20 μm) was completely consumed, and another ternary compound, τ_2-Ti_2AlN, began to form between τ_1-Ti_3AlN and α_2-Ti_3Al. Han *et al.*[12] stated that δ-TiN and τ_1-Ti_3AlN were present in the reaction zone after AlN/Ti (150 μm)/AlN sandwiched specimens were annealed at 1000°C for 200 h in a vacuum.

Several researchers have investigated the AlN/Ti interfacial reactions in bulk or powder.[12–15] Paransky *et al.*[13–15] found that δ-TiN, τ_1-Ti_3AlN, and α_2-Ti_3Al were formed between AlN (powder) and Ti (powder) after annealing at 900°–1100°C for 1–40 h. A lamellar (α_2-Ti_3Al+τ_1-Ti_3AlN) layer was observed between τ_1-Ti_3AlN and α_2-Ti_3Al after annealing at 1000° or 1100°C. Han *et al.*[12] observed δ-TiN, τ_1-Ti_3AlN, and α_2-Ti_3Al after the mixtures of AlN and Ti powders (AlN:Ti = molar ratio of 1:2) were annealed at 1000°C for 200 h under vacuum. However, the crystallographic relationships and mechanisms of phase transformation among these phases have not yet been fully explored.

As Table I indicates, X-ray diffraction (XRD) and scanning electron microscopy/energy-dispersive spectrometry (SEM/EDS) are most frequently used to investigate the AlN/Ti interface. However, chemical SEM/EDS analyses and crystallographic XRD analyses are based on microscopic and macroscopic scales, respectively.[14] In addition, SEM/EDS analysis is complicated by the coexistence of several binary and ternary phases with similar compositions (Ti_3AlN, Ti_3AlN_{1-x}, Ti_2AlN, Ti_2N, and TiN_{1-x}) and by the overlap of titanium (Ti) *L* and nitrogen (N) *K* spectral series.[14] As a result, the combination of XRD and SEM/EDS does not allow for full characterization of the AlN/Ti interface.

Recently, Paransky *et al.*[13–15] investigated the AlN–Ti interface using the electron backscatter diffraction (EBSD) attached to the SEM. One major advantage of the EBSD technique is its ability to provide crystallographic information, which is supplementary to traditional SEM/EDS analyses. However, the EBSD can only be operated over a very limited range of incident angles, and cannot provide resolution on a submicrometer scale, such as a fine precipitate and/or a fine lamellar structure at the AlN–Ti interface.

Selected electron diffraction patterns can be conducted over a wide range of incident angles and on a submicrometer scale using a transmission electron microscope (TEM). Because TEM/EDS can provide simultaneous microstructural observation, crystallographic and compositional analyses with good resolution, it is a much more effective tool for microstructural characterization than methods such as SEM/EDS, XRD, and EBSD. However, TEM/EDS has only been applied to the investigation of the AlN/Ti interface in very few studies[6,8] because it is very challenging to prepare the cross-sectional TEM specimens.

Recently, Chiu and Lin[16] proposed the phase formation mechanisms in the AlN/Ti diffusion couple at 1300°–1500°C based on microstructural characterization using TEM/EDS and SEM/EDS. An interfacial reaction zone, consisting of δ-TiN, τ_2-Ti_2AlN, τ_1-Ti_3AlN, α_2-Ti_3Al, and a two-phase (α_2-Ti_3Al+α-Ti) region in sequence, was observed in the AlN/Ti diffusion couple after annealing at 1300°C. The γ-TiAl and a lamellar two-phase (γ-TiAl+α_2-Ti_3Al) structure were present between τ_2-Ti_2AlN and α_2-Ti_3Al after annealing at 1400°C, while no γ-TiAl was present at the interface after annealing at 1500°C.

In this work, TEM/EDS was utilized to examine the phase evolution of the interfacial reaction zone between AlN and Ti after annealing at 1000°C for 0.1–36 h in an Ar atmosphere. The

H. Chan—contributing editor

Manuscript No. 23624. Received August 17, 2007; approved December 11, 2007.
*Member, The American Ceramic Society.
†Author to whom correspondence should be addressed. e-mail: chienlin@faculty.nctu.edu.tw

Table I. Summary of Some Previous Studies on the AlN/Ti Interfacial Reactions

Type of samples	Annealing conditions	Analyzing instruments	Reaction products	References
Ti thick film/AlN thin film or substrate	Annealing at 600°–800°C for a short time	XRD, XPS, RBS, and TEM	$TiAl_3$–TiN–Ti_4N_{3-x}–Ti_2N	He *et al.*[7]
Ti thin film/AlN substrate	Annealing at 600°–950°C for 2–30 min	RBS, XRD, and TEM	Ti_2AlN	Imanaka and Notis[6]
Ti thin film/AlN thin film	Annealing at 600°C for 1–10 h in N_2	AES, XRD, and TEM	$TiAl_3$–Ti_2N–Ti_3Al–α-$(Ti, Al)_{ss}$	Pinkas *et al.*[8]
Ti thin film/AlN substrate	Annealing at 700°–950°C for 60 min	XRD	$TiAl_3$, Ti_2N, TiN	Yasumoto *et al.*[9]
Ti thin film/AlN substrate	Annealing at 200°–850°C for 1–4 h	SIMS, RBS, and XRD	$TiN_{0.3}$, $Ti_3Al_2N_2$, Ti_2AlN, Ti_3Al, TiN and Ti_2N	Yue *et al.*[10]
Ti foil/AlN substrate	Annealing at 1050°–1200°C for 2–20 h in vacuum	XRD, SEM, and EPMA	TiN–Ti_3AlN–Ti_3Al	El-Sayed *et al.*[11]
Ti foil and AlN bulk	Annealing at 1000°C for 200 h	SEM, XRD, and EPMA	TiN–Ti_3AlN	Han *et al.*[12]
Ti powder and AlN powder	Annealing at 1000°C for 200 h	SEM, XRD, and EPMA	TiN–Ti_3AlN–Ti_3Al	Han *et al.*[12]
Ti powder and AlN powder	Annealing at 900° and 1100°C for 1–40 h	SEM/EDS/EBSD, XRD, and EPMA	TiN–Ti_3AlN–lamellar (Ti_3AlN+Ti_3Al)–Ti_3Al	Paransky *et al.*[13–15]
Ti bulk and AlN bulk	Annealing at 900° and 1100°C for 1–40 h	SEM/EDS/EBSD, XRD, and EPMA	TiN–Ti_3AlN–lamellar (Ti_3AlN+Ti_3Al)–Ti_3Al	Paransky *et al.*[15]
Ti powder and AlN bulk	Annealing at 900° and 1100°C for 1–40 h	SEM/EDS/EBSD, XRD, and EPMA	TiN–$(Ti)_{Ak}$	Paransky *et al.*[15]
Ti bulk and AlN bulk	Annealing at 1300°–1500°C/0.5–36 h	SEM/EDS and TEM/EDS	TiN–Ti_2AlN–Ti_3AlN–Ti_3Al–two-phase (Ti_3Al+Ti) at 1300°C TiN–Ti_2AlN–TiAl–lamellar (TiAl+Ti_3Al)–Ti_3Al–two-phase (Ti_3Al+Ti) at 1400°C TiN–Ti_2AlN–lamellar (TiAl+Ti_3Al)–Ti_3Al–two-phase (Ti_3Al+Ti) at 1500°C	Chiu and Lin[16]

interfacial reactions for various periods are described in terms of diffusion paths, which are depicted in an isothermal Al–N–Ti ternary phase diagram. The crystallographic relationships and phase transformation mechanisms of δ-TiN, τ_1-Ti_3AlN, and α_2-Ti_3Al are also elucidated.

II. Experimental Procedure

AlN plates (SH-15, with a nominal composition of 62.8% Al, 32.1% N, 3.4% Y, 1.7% O, Tokuyama Soda Corp., Tokyo, Japan) and commercially pure Ti billets (99.7% purity, Alfa Aesar, Ward Hill, MA) were cut into pieces with dimensions of approximately 15 mm × 10 mm × 4 mm. Using a precision polishing machine (Model Minimet 1000, Buehler Ltd., Lake Bluff, IL), all of the pieces were ground with a 15 μm diamond matted disk and then polished with 3 μm diamond paste and a 1 μm alumina suspension. After they were rinsed ultrasonically in an acetone bath and distilled water, the sandwiched samples, with the Ti metal placed between two pieces of AlN, were annealed under a low pressure of 2 MPa at 1000°C for various periods in an atmosphere of argon (with $O_2 < 1$ ppm, $H_2O < -76$ ppm/°C, THC < 0.5 ppm, and $N_2 < 3$ ppm).

A slice with a thickness of approximately 300 μm was cut from each annealed sample perpendicular to the interface of AlN and Ti. The slice was then ground and polished down to a thickness of 80–100 μm following the standard metallographic procedures described above. Each metallographic sample was etched using the Kroll reagent (10 mL HF+30 mL HNO_3+60 mL H_2O) for SEM/EDS analyses. The cross-sectional slab was further thinned to a thickness of 20–30 μm by dimpling, and was finally argon-ion milled at 5 kV and 20 μA for TEM/EDS analyses.

The AlN/Ti interfacial microstructures were characterized using a transmission electron microscope (Model 2000FX, JEOL, Tokyo, Japan) and a scanning electron microscope (Model JSM-6500, JEOL, Tokyo, Japan), both equipped with an ultra-thin window EDS detector (Model 9900, EDAX International, Prairie View, IL). The Cliff–Lorimer standardless technique was applied to analyze the compositions of various phases at the thin edge of the TEM samples.

III. Results and Discussion

(1) Microstructures of the AlN/Ti Interface

Figure 1 illustrated the variation in the interfacial microstructures of AlN and Ti after annealing at 1000°C for various periods. Figure 1(a) presented the secondary electron image of the cross section of the AlN/Ti interface after annealing at 1000°C/0.1 h, revealing that the reaction zone consisted of one well-defined reaction layer, which was identified as δ-TiN with <2 at.% Al in solid solution. A similar result was also demonstrated in previous works.[17,18] Figure 1(b) displayed the

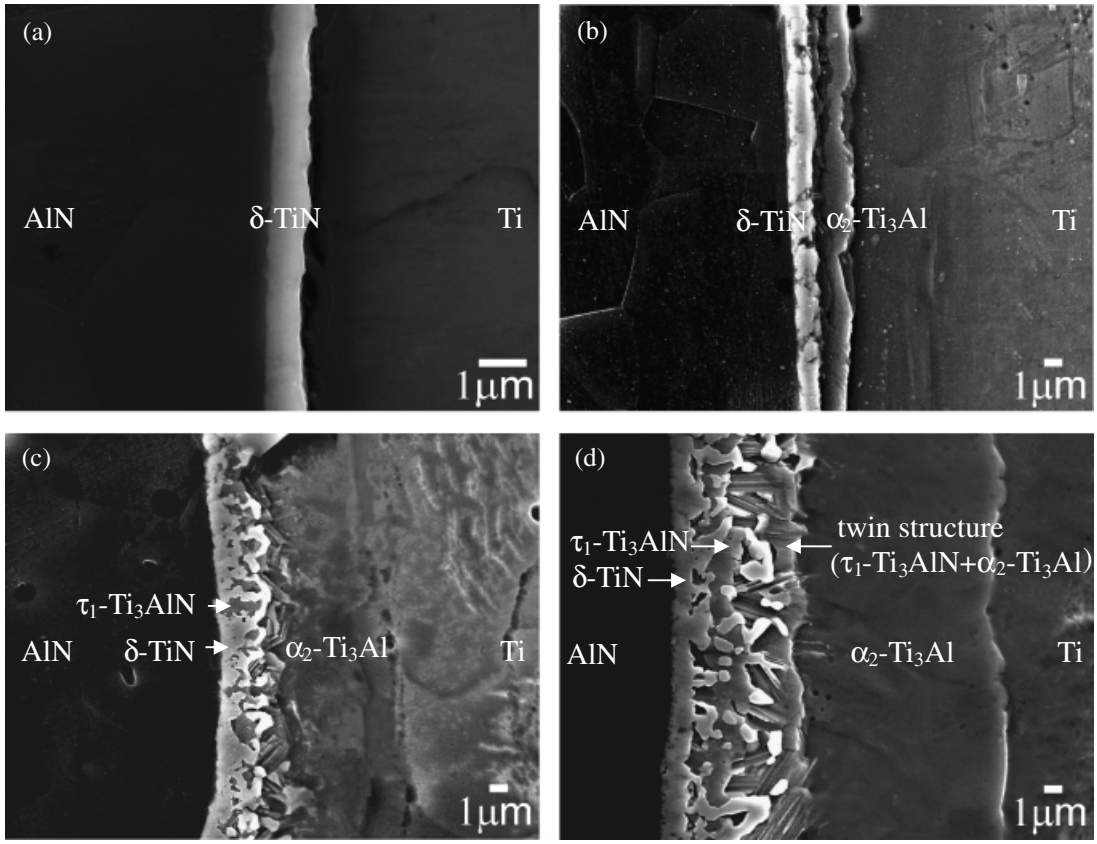

Fig. 1. Scanning electron micrographs showing the AlN/Ti interfaces after annealing at 1000°C for (a) 0.1 h; (b) 0.5 h; (c) 3 h; and (d) 36 h, respectively.

interfacial reaction zone of AlN/Ti after annealing at 1000°C/0.5 h, indicating the presence of δ-TiN and α_2-Ti_3Al at the AlN/Ti interface. Some investigations[7,8,19] have reported that δ-TiN and $TiAl_3$ are initially formed at the AlN/Ti interface after annealing between 600° and 800°C. Pinkas *et al.*[8] investigated the early stage of interface reactions between AlN and Ti thin films at 600°C for 1–10 h, indicating that the phase sequence was AlN/$TiAl_3$/Ti_2N/Ti_3Al/α-$(Ti, Al)_{ss}$. However, $TiAl_3$ was not observed in the reaction zone between AlN and Ti after annealing at 1000°C/0.5 h, as shown in Fig. 1(b). Figure 1(c) revealed that the insular τ_1-Ti_3AlN began to precipitate in the δ-TiN layer after annealing at 1000°C/3 h. The τ_1-Ti_3AlN in the δ-TiN layer became interconnected during annealing at 1000°C/36 h, as displayed in Fig. 1(d). Moreover, the twinned structure (τ_1-Ti_3AlN+α_2-Ti_3Al) and insular δ-TiN were present at the interface between δ-TiN and α_2-Ti_3Al after annealing at 1000°C/36 h. The insular δ-TiN grains, mentioned above, appeared as the brightest phase in Fig. 1(d). It was believed that the formation of the twinned structure (τ_1-Ti_3AlN+α_2-Ti_3Al) and insular δ-TiN was caused by the nitridization of the α_2-Ti_3Al layer, as discussed below in detail. The comparison between Figs. 1(c) and (d) revealed that the δ-TiN layer hardly grew at the AlN/Ti interface at 1000°C, although the thickness of the α_2-Ti_3Al layer increased with annealing time.

According to the Ti–Al–N ternary phase diagram at 1000°C, ternary compounds such as τ_1-Ti_3AlN and τ_2-Ti_2AlN exist in the equilibrium system. Han *et al.*[12] reported that the formation energies of τ_1-Ti_3AlN and τ_2-Ti_2AlN at 1000°C were −360 and −323 kJ/mol, respectively, revealing that their formation was thermodynamically favorable. Magnan *et al.*[21] indicated that α_2-Ti_3Al could be nitridized to τ_1-Ti_3AlN upon annealing at 1000°C, and τ_1-Ti_3AlN was gradually replaced by τ_2-Ti_2AlN with time. However, no τ_2-Ti_2AlN was found in this study. Only limited Al and N atoms diffused through δ-TiN to react with α_2-Ti_3Al in the AlN/Ti diffusion couple. This prohibited the further formation of any Al- and N-rich phase, e.g., τ_2-Ti_2AlN, in the AlN/Ti diffusion couple.

As mentioned above, τ_1-Ti_3AlN was formed at the grain boundaries of the δ-TiN layer during annealing at 1000°C/3 h [Fig. 1(c)], and became interconnected during annealing at 1000°C/36 h [Fig. 1(d)]. Figure 2(a) revealed that the residual δ-TiN was embedded in the growing τ_1-Ti_3AlN during annealing at 1000°C/10 h, suggesting that the τ_1-Ti_3AlN grew as the δ-TiN layer was consumed. The lattice parameter of τ_1-Ti_3AlN deviated from that of δ-TiN by $<3\%$ ($a = 4.24$ nm for δ-TiN and $a = 4.11$ nm for τ_1-Ti_3AlN). The selected area diffraction patterns (SADPs) of τ_1-Ti_3AlN and δ-TiN were distinguished by whether the superlattice diffractions were present in the SADPs, as shown in Figs. 2(b) and (c). No superlattice diffractions such as (110) and (101) were present in the SADPs of the δ-TiN with the NaCl-like structure, while the SADPs of the τ_1-Ti_3AlN were typical (001)* patterns for the pervoskite-like structure, revealed by the superlattice diffractions (100), (010), (110), and others. The SADPs in Fig. 2(d) revealed that the orientation relationships of δ-TiN and τ_1-Ti_3AlN were $[111]_{\tau_1\text{-}Ti_3AlN}//[111]_{\delta\text{-}TiN}$ and $(1\bar{1}0)_{\tau_1\text{-}Ti_3AlN}//(1\bar{1}0)_{\delta\text{-}TiN}$. Both δ-TiN and τ_1-Ti_3AlN could be discernible based upon elemental quantitative analyses using TEM/EDS because δ-TiN dissolved a very limited amount of Al ($\approx$0.3 at.%) and τ_1-Ti_3AlN contained approximately 20 at.% Al, as shown in Figs. 2(e) and (f), respectively. From the crystallographic viewpoint, the phase transformation from δ-TiN to τ_1-Ti_3AlN can be understood as follows: one Ti atom (at a corner) in a unit cell of δ-TiN was replaced by Al and three N atoms (at the octahedral interstitial sites) were evolved, based upon the following chemical reaction:

$$4\delta\text{-TiN} + Al \rightarrow \tau_1\text{-}Ti_3AlN + 3N + Ti \quad (1)$$

Paransky *et al.*[13–15] alleged that a lamellar structure was present at the interface between AlN and Ti powders after annealing at 900°–1100°C for 1–40 h, revealing that the τ_1-Ti_3AlN phase precipitated from supersaturated α_2-Ti_3Al with N in solid solution during cooling. However, Fig. 3(a) revealed that the system existed as a twinned rather than lamellar structure after

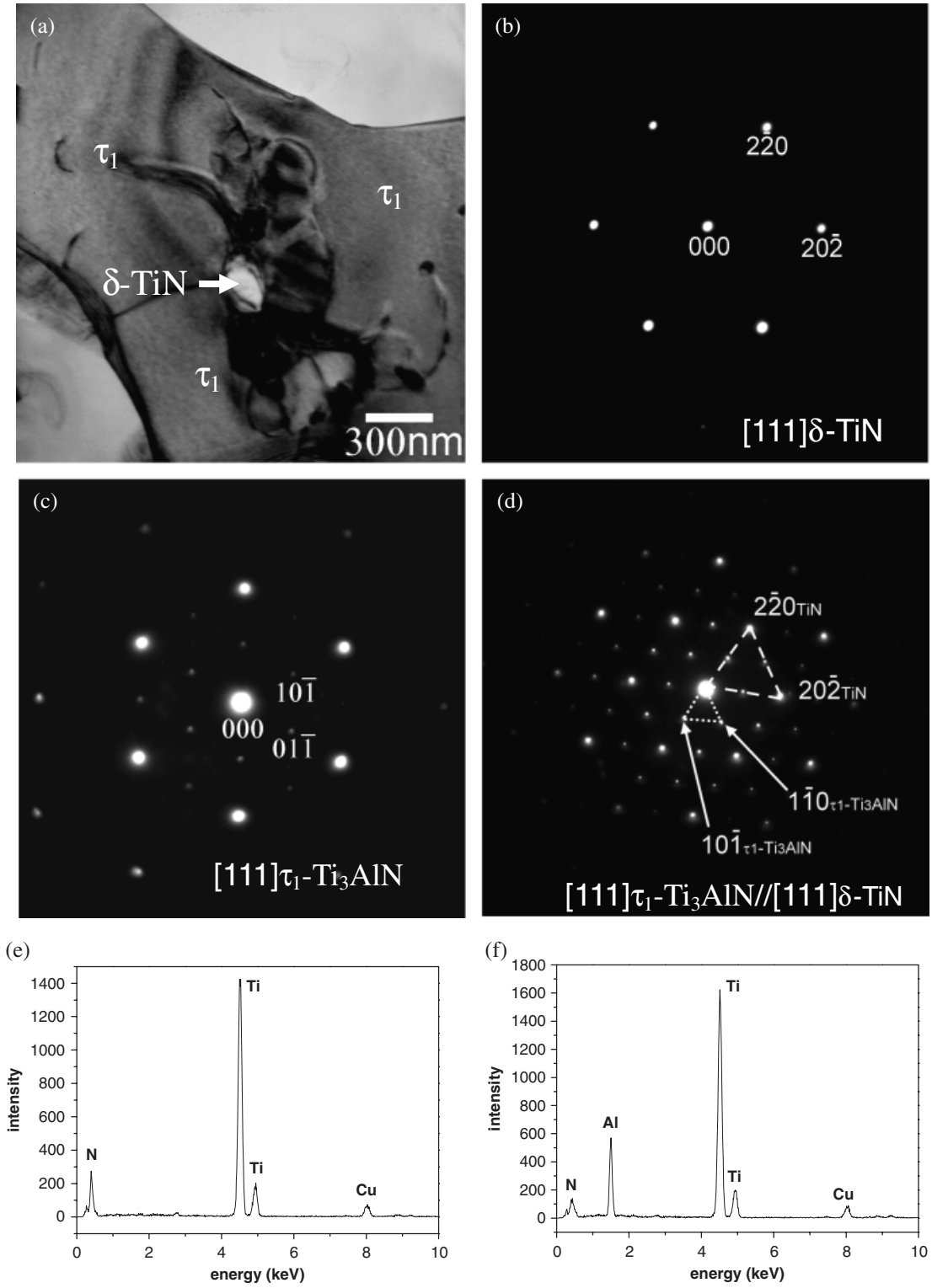

Fig. 2. (a) A bright-field image of the residual δ-TiN phase in τ_1-Ti_3AlN after annealing at 1000°C/10 h; (b) an SADP of δ-TiN, $z = [111]$; (c) an SADP of τ_1-Ti_3AlN, $z = [001]$; (d) the SADPs of τ_1-Ti_3AlN and δ-TiN, showing the orientation relationships of $[111]_{\tau_1\text{-}Ti_3AlN}//[111]_{\delta\text{-}TIN}$ and $(1\bar{1}0)_{\tau_1\text{-}Ti_3AlN}//(1\bar{1}0)_{\delta\text{-}TiN}$; (e) the EDS spectrum of δ-TiN; (f) the EDS spectrum of τ_1-Ti_3AlN. SADP, selected area diffraction pattern; EDS, energy-dispersive spectrometry.

annealing at 1000°C/10 h. Figure 3(b) displayed the superimposed SADPs of α_2-Ti_3Al ($z = [1\bar{1}01]$)and τ_1-Ti_3AlN ($z = [011]$), with the electron beam in the edge-on direction of the twin plane $(01\bar{1}1)_{\alpha_2\text{-}Ti_3Al}$. The twinned structure was implied by the streaking of the diffraction spots along the direction perpendicular to the twin plane and the presence of extra spots symmetrical with respect to the twin plane in the SADPs, as shown in Fig. 3(b). For clarity, the superimposed SADPs in Fig. 3(b) were redrawn and indexed in Fig. 3(c). The superimposed SADPs, shown in Figs. 3(b) and (d), clearly illustrated that the twinned structure contained two phases, identified as hcp ordered α_2-Ti_3Al and cubic τ_1-Ti_3AlN, respectively, and that they were orientated with the relationships $[111]_{\tau_1\text{-}Ti_3AlN}//[001]_{\alpha_2\text{-}Ti_3Al}$ and $(0\bar{1}1)_{\tau_1\text{-}Ti_3AlN}//(\bar{1}\bar{1}20)_{\alpha_2\text{-}Ti_3Al}$.

Figures 4(a) and (b) presented the bright-field image and central dark-field image (CDFI), respectively, of the twinned

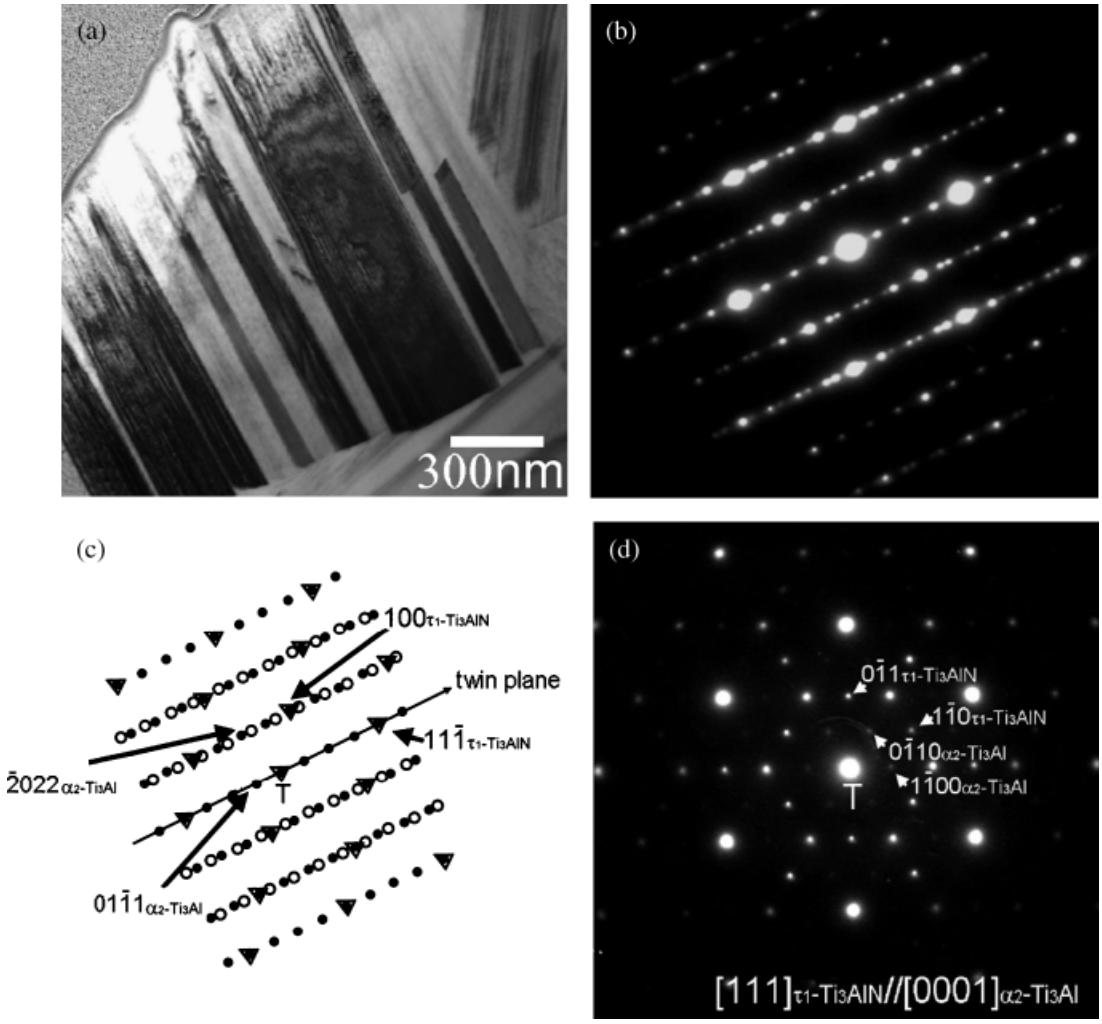

Fig. 3. After annealing at 1000°C/10 h: (a) the bright-field image of the (τ_1-Ti_3AlN+α_2-Ti_3Al) twinned structure; (b) the selected area diffraction patterns (SADPs) of τ_1-Ti_3AlN ($z=[1\bar{1}01]$) and α_2-Ti_3Al ($z=[011]$) with the orientation relationships $[011]_{\tau_1\text{-}Ti_3AlN}//[1\bar{1}01]_{\alpha_2\text{-}Ti_3Al}$ and $(100)_{\tau_1\text{-}Ti_3AlN}//(1\bar{1}02)_{\alpha_2\text{-}Ti_3Al}$; (c) the schematic illustration of the SADPs in (b) (●, α_2-Ti_3Al matrix; ○, α_2-Ti_3Al twin; Δ, τ_1-Ti_3AlN); (d) the SADPs of τ_1-Ti_3AlN ($z=[111]$) and α_2-Ti_3Al ($z=[0001]$) with the orientation relationships $[111]_{\tau_1\text{-}Ti_3AlN}//[0001]_{\alpha_2\text{-}Ti_3Al}$ and $(0\bar{1}1)_{\tau_1\text{-}Ti_3AlN}//(\bar{1}120)_{\alpha_2\text{-}Ti_3Al}$.

structure as shown in Fig. 3(a). The bands of the twin and the matrix were somewhat discernible while comparing Figs. 4(a) and (b) with Fig. 3(a). The CDFI was formed by the diffraction spot $(0\bar{1}10)$ of α_2-Ti_3Al such that the α_2-Ti_3Al phase appeared bright in Fig. 4(b). Two phases appeared to be present and the chopped fiber-like α_2-Ti_3Al was aligned with τ_1-Ti_3AlN in the direction perpendicular to the twin plane.

The mechanism of phase transformation from α_2-Ti_3Al to τ_1-Ti_3AlN could be seen with the help of Fig. 5. The ordering of N atoms was responsible for the formation of τ_1-Ti_3AlN.

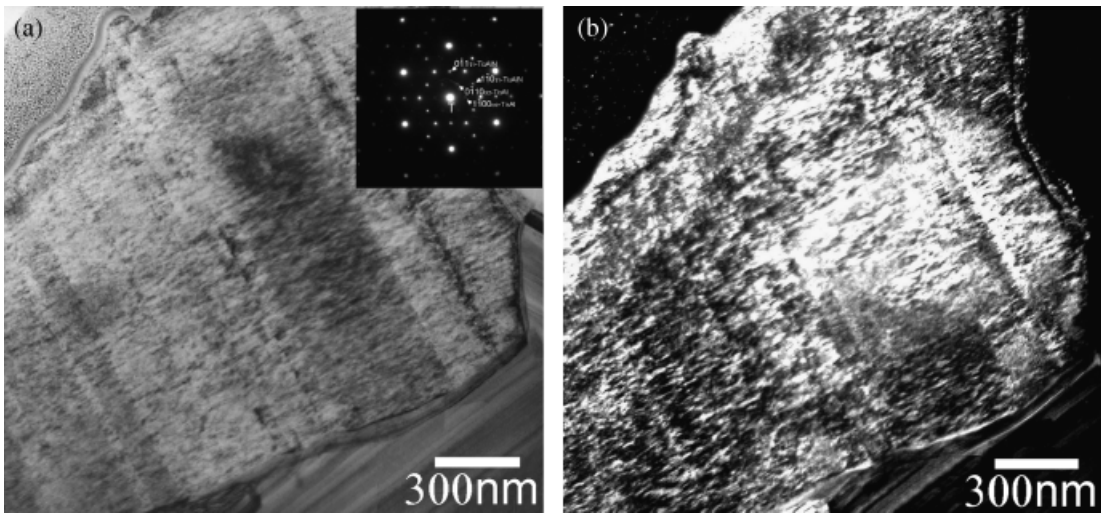

Fig. 4. After annealing at 1000°C/10 h: (a) the bright-field image of the (τ_1-Ti_3AlN+α_2-Ti_3Al) twinned structure; (b) the central dark-field (CDF) image of the (τ_1-Ti_3AlN+α_2-Ti_3Al) twinned structure formed by the diffraction spot $(0\bar{1}10)$ of α_2-Ti_3Al.

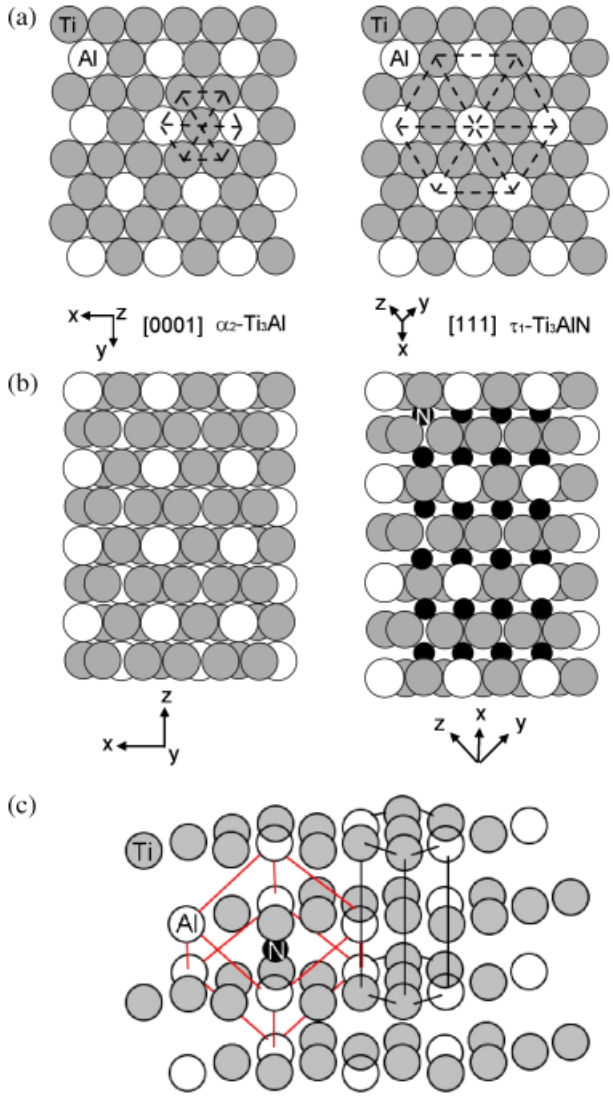

Fig. 5. (a) Crystal structures of α_2-Ti_3Al and τ_1-Ti_3AlN projected along the $[0001]_{\alpha\text{-}Ti_3Al}$ or $[111]_{\tau_1\text{-}Ti_3AlN}$ direction; (b) the stacking sequence of closely packed planes viewed along $[01\bar{1}0]_{\alpha_2\text{-}Ti_3Al}$ or $[1\bar{2}1]_{\tau_1\text{-}Ti_3AlN}$; (c) the lattice relationship of the cubic τ_1-Ti_3AlN (red line) and the hexagonal α_2-Ti_3Al (black line).

At high temperatures, α_2-Ti_3Al could dissolve a significant amount of N atoms, which occupied one of the octahedral interstitial sites of α_2-Ti_3Al in an orderly manner during cooling. The crystal structures of α_2-Ti_3Al and τ_1-Ti_3AlN were hexagonal and pervoskite, respectively. The most closely packed {0001} planes of α_2-Ti_3Al and the most closely packed {111} planes of τ_1-Ti_3AlN were parallel based on the SADPs in Fig. 3(d). The {0001} interlayer distance of hexagonal α_2-Ti_3Al was calculated as $c/2$ or 0.233 nm, while the {111} interlayer distance of cubic τ_1-Ti_3AlN was calculated as the diagonal length $\sqrt{3}a$ divided by 3 or 0.237 nm. The equality of their closely packed interlayer distances was consistent with the crystallographic relationships mentioned above. The closely packed planes of α_2-Ti_3Al and τ_1-Ti_3AlN, lying in the plane of the paper, could be seen in Fig. 5(a) along the $[0001]_{\alpha_2\text{-}Ti_3Al}$ or $[111]_{\tau_1\text{-}Ti_3AlN}$, while the stacking sequences of closely packed planes in Fig. 5(b) were viewed along $[01\bar{1}0]_{\alpha_2\text{-}Ti_3Al}$ or $[1\bar{2}1]_{\tau 1\text{-}Ti_3AlN}$. Although Ti and Al atoms were not redistributed during the phase transformation, N atoms were inserted between two neighboring closely packed planes. Figure 5(c) presented the crystallographic relationships between pervoskite τ_1-Ti_3AlN (red line, with Al atoms at corners, Ti at face-center positions, and N at body-center positions) and hexagonal α_2-Ti_3Al (black line), indicating that

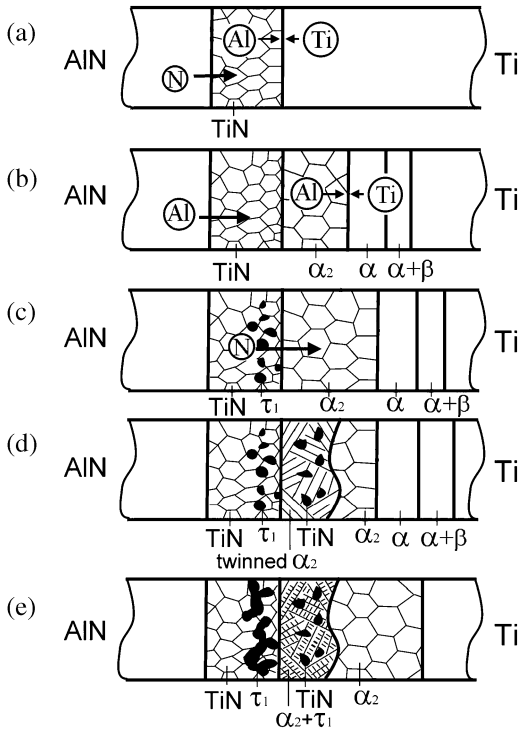

Fig. 6. Microstructural development in the AlN/Ti diffusion couple after annealing at 1000°C for 0.1–36 h; (a) formation of the δ-TiN layer; (b) formation of the α_2-Ti_3Al layer and various titanium aluminides; (c) formation of τ_1-Ti_3AlN in the δ-TiN layer; (d) formation of δ-TiN and twinned α_2-Ti_3Al due to the nitridization of the α_2-Ti_3Al layer; (e) formation of the τ_1-Ti_3AlN+α_2-Ti_3Al twinned structure during cooling.

N atoms occupied one of the octahedral interstitial sites of α_2-Ti_3Al in an orderly manner during cooling.

(2) Microstructural Development of the AlN/Ti Interface

The microstructural development at the AlN/Ti interface at temperatures from 1300° to 1500°C has been described elsewhere.[16] Very different microstructures were obtained after annealing at 1000°C, and the reactions and phase formations at the interface between AlN and Ti at 1000°C are described in the following sections.

(A) Stage 1: Formation of the δ-TiN Layer: The formation mechanism of the δ-TiN layer has been described in a previous study,[16] and is again schematically illustrated in Fig. 6(a). According to the Ti–N binary phase diagram,[22] α-Ti is stable with up to 23 at.% N in solid solution at 1000°C, beyond which there exists a two-phase (α-Ti+δ-TiN) region in the range of 23–30 at.% N. This implies that the δ-TiN is not formed until more than 23 at.% N is dissolved in α-Ti at 1000°C. The δ-TiN phase, with an NaCl-like structure, has a nonstoichiometric composition (designated as $\delta\text{-}TiN_{1-x}$) in the wide range of 30–55 at.% N. The δ-TiN layer can be thought of as a N sponge that responds to diffusing N atoms in the same way as a sponge responds to water. Essentially, the δ-TiN layer can also be regarded as a "trap" or a "garbage can" for N atoms at this stage, explaining why the δ-TiN layer growth at the AlN/Ti interface is not evident at 1000°C.

(B) Stage 2: Formation of the α_2-Ti_3Al Layer: Because the solubility of Al in δ-TiN is rather limited, Al atoms are not dissolved in the δ-TiN layer but diffuse through the δ-TiN layer into Ti, resulting in the formation of α_2-Ti_3Al between δ-TiN and Ti in the second stage, as displayed in Fig. 6(b). Excess Al atoms may proceed further beyond the α_2-Ti_3Al layer into Ti, forming an α-Ti(Al) solid solution and probably a two-phase region (α-Ti+β-Ti), according to the Ti–Al–N ternary phase diagram.[19] While Al or N atoms diffuse into β-Ti (A2, bcc)

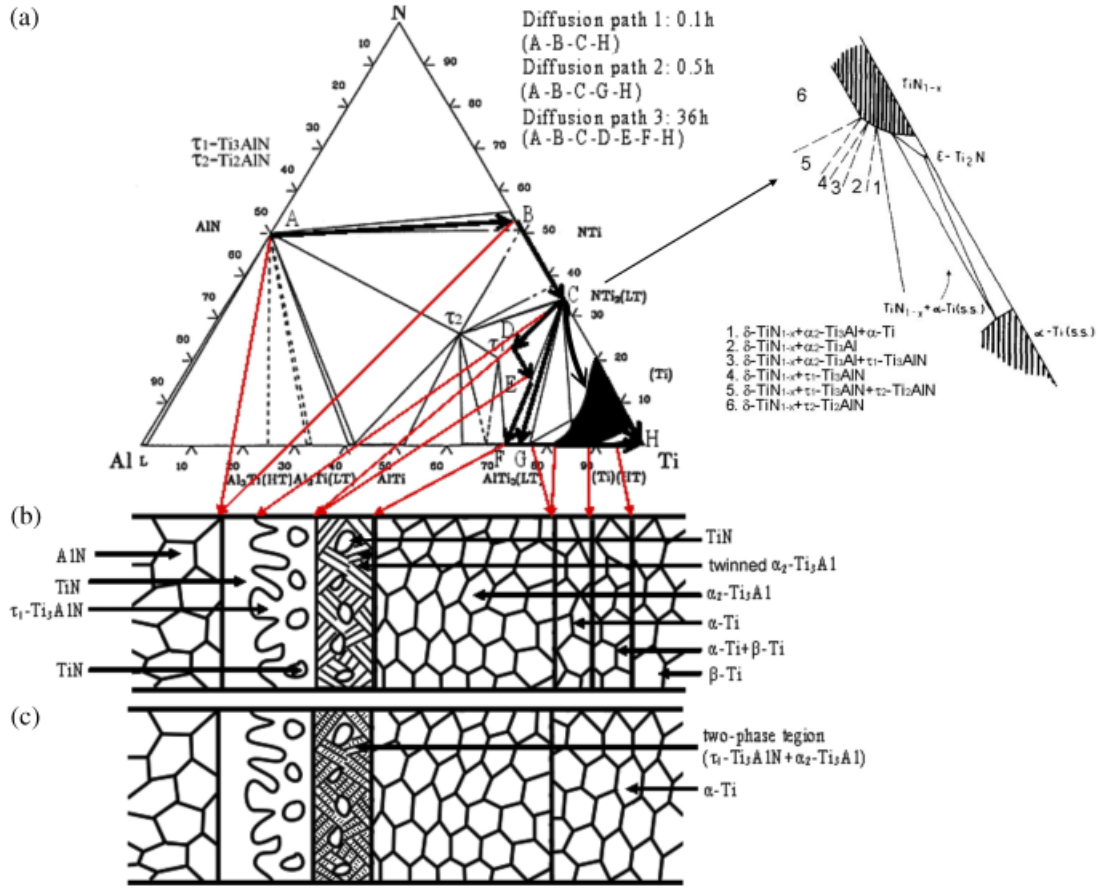

Fig. 7. (a) An isothermal section of the Ti–Al–N system at 1000°C, and the diffusion paths (path 1: A→B→C→H for 0.1 h; path 2: A→B→C→G→H for 0.5 h; path 3: A→B→C→D→E→F→G→H for 36 h); (b) schematic microstructure at the AlN/Ti interface on annealing at 1000°C/36 h; (c) schematic microstructure of the AlN/Ti interface after cooling.

during annealing at 1000°C, the dissolution of up to 5 at.% Al and/or N atoms makes α-Ti (A3, hcp) relatively stable with respect to β-Ti. The α_2-Ti_3Al grows if more than 23 at.% Al is dissolved in α-Ti at 1000°C.

(C) Stage 3: Formation of τ_1-Ti_3AlN in the δ-TiN Layer: Following the formation of α_2-Ti_3Al, some Al atoms tend to accumulate at the δ-TiN grain boundaries and then react with δ-TiN to form τ_1-Ti_3AlN, as shown in Fig. 6(c). The τ_1-Ti_3AlN gradually becomes continuous over a long period. The formation of intergranular τ_1-Ti_3AlN in δ-TiN is given by the chemical reaction (1) mentioned above.

The aluminization of the δ-TiN layer gives rise to the formation of intergranular τ_1-Ti_3AlN accompanied with the exsolution of N. The τ_1-Ti_3AlN is expected to be generated by the nitridization of the α_2-Ti_3Al layer previously formed, but in this stage, the formation obviously proceeds through a different mechanism.

(D) Stage 4: Formation of δ-TiN and Twinned α_2-$Ti_3Al(N)$ in the α_2-Ti_3Al Layer: The excess N atoms, as described by reaction (1), diffuse into the α_2-Ti_3Al layer and react with α_2-Ti_3Al to become the α_2-$Ti_3Al(N)$ solid solution. As the concentration of N atoms increases, the twinning of α_2-$Ti_3Al(N)$ is triggered, as shown in Fig. 3(a). The nitridization of α_2-Ti_3Al also generates δ-TiN in the α_2-Ti_3Al layer, because N atoms have a high affinity to Ti atoms [Fig. 6(d)].

The small interstitial atoms, such as N and hydrogen, behave very similarly when they are dissolved in α_2-Ti_3Al. Xiao *et al.*[22] stated that at 373–473 K, deuterium was readily dissolved in α_2-Ti_3Al as a solid solution and that increasing the deuterium concentration to $D/\alpha_2\text{-}Ti_3Al \geq 0.18$ caused the twinning of deuteride with DO_{19}. Additionally, $\delta\text{-}Ti_3AlD_x$ and twinned deuteride coexisted at $D/\alpha_2\text{-}Ti_3Al \geq 0.59$. It is believed that the phase transformation induced by the dissolution of N atoms in α_2-Ti_3Al corresponds to that induced by the dissolution of deuterium in α_2-Ti_3Al. In this study, the twinned structure was first found in the literature at the AlN-Ti interface, and it is comparable to the twinned deuteride in α_2-Ti_3Al as $D/\alpha_2\text{-}Ti_3Al \geq 0.59$.

(E) Stage 5: Formation of τ_1-Ti_3AlN in Twinned α_2-$Ti_3Al(N)$ During Cooling: The high-temperature α_2-$Ti_3Al(N)$ solid solution undergoes an incongruent phase transformation or phase separation during cooling, yielding a high-N phase and a low-N phase. The N atoms in the low-N phase or α_2-$Ti_3Al(N)$ are randomly distributed in an hcp crystal structure, whereas the N atoms in the high-N phase or τ_1-Ti_3AlN occupy one of the octahedral interstitial sites in each unit cell. τ_1-Ti_3AlN and α_2-Ti_3Al have very similar crystal structures, and their crystallographic relationships are as shown in Fig. 5(c). However, the composition of τ_1-Ti_3AlN (60.1 at.% Ti, 19.9 at.% Al, and 20.0 at.% N) differs substantially from that of α_2-$Ti_3Al(N)$ (71.5 at.% Ti, 23.2 at.% Al, and 5.3 at.% N). Notably, the twinning of α_2-Ti_3Al occurs before τ_1-Ti_3AlN is formed, because the twinning will not take place across different phases. Figure 6(e) schematically depicts the final microstructure developed at the AlN/Ti interface after cooling.

(3) Diffusion Path in the Ti–Al–N Ternary Phase Diagram

The microstructural development at the AlN/Ti interface is related to the diffusion path in the isothermal section of the Al–N–Ti ternary phase diagram.[23] Figure 7(a) presents three diffusion paths, represented by the arrowed lines on the isothermal Ti–Al–N phase diagram, in the AlN/Ti diffusion couple upon annealing at 1000°C for various periods. Based on the experimental results, when the diffusion couples of AlN and Ti are isothermally annealed at 1000°C, the diffusion paths as-

sociated with the compositions along the longitudinal direction perpendicular to the interface are proposed as follows: (a) A→B→C→H (path 1) for 0.1 h; (b) A→B→C→G→H (path 2) for 0.5 h; and (c) A→B→C→D→E→F→G→H (path 3) for 36 h. It is noted that all diffusion paths do not go through Ti_2N based on the present results. A magnified section of the Ti–Al–N ternary phase diagram proposed by Schuster and Bauer[18] is redrawn in the upper right-hand corner of Fig. 7(a), indicating the coexistence of δ-TiN with τ_1-Ti_3AlN and/or α_2-Ti_3Al in an equilibrium state at 1000°C. For the case of annealing at 1000°C/36 h, the diffusion path crosses the fields AlN+δ-TiN, δ-TiN, δ-TiN+τ_1-Ti_3AlN, δ-TiN+τ_1-Ti_3AlN+α_2-Ti_3Al, δ-TiN+α_2-Ti_3Al, α_2-Ti_3Al, α_2-Ti_3Al+α-Ti, α-Ti, β-Ti+α-Ti, and β-Ti between AlN and Ti. The three-phase region and the tie lines in the two-phase region correspond to the interface between the two reaction layers in the diffusion couple.

Figures 7(b) and (c) present the microstructures that developed in the AlN/Ti diffusion couples upon annealing at 1000°C/36 h and subsequent cooling, respectively. The connecting lines delineate the relationship between the microstructure [Fig. 7(b)] and the isothermal section of the Ti–Al–N phase diagram [Fig. 7(a)]. As displayed in Fig. 7(b), the layers of δ-TiN, δ-TiN+τ_1-Ti_3AlN, δ-TiN+twinned α_2-Ti_3Al, α_2-Ti_3Al, and Ti (α-Ti, β-Ti+α-Ti, β-Ti, etc.) were formed in sequence from AlN to Ti upon annealing at 1000°C/36 h. Figure 7(c) shows the final microstructure, indicating that the twinned α_2-Ti_3Al was transformed to the (α_2-Ti_3Al+τ_1-Ti_3AlN) structure from the two-phase region (δ-TiN+α_2-Ti_3Al) during subsequent cooling. β-Ti and β-Ti+α-Ti were absent between α_2-Ti_3Al and α-Ti after cooling, because β-Ti was transformed to α-Ti at the phase transformation temperature (883°C) upon cooling. For other annealing periods, the relationship between microstructural development and diffusion path can be explained in a similar way.

Based on the foregoing discussion, it was worth mentioning that some new findings were obtained in the present study. For example, the phase transformation and orientation relations were definitely recognized between δ-TiN and τ_1-Ti_3AlN (or between α_2-Ti_3Al and τ_1-Ti_3AlN) at the AlN/Ti interface on behalf of TEM/EDS works. For the first time, it revealed a twinned α_2-Ti_3Al structure on annealing at 1000°C/10 h, while an ordered cubic τ_1-Ti_3AlN was precipitated from the twinned α_2-Ti_3Al during cooling. This study also illustrated the phase transformation mechanism from α_2-Ti_3Al to τ_1-Ti_3AlN due to the interdiffusion in the AlN/Ti diffusion couple from a crystallographic viewpoint.

IV. Conclusions

1. The microstructures of various reaction layers in the AlN/Ti diffusion couples after annealing at 1000°C were thoroughly investigated using analytical SEM and TEM.

2. In the initial stages, one δ-TiN layer was formed between AlN and Ti, and then a α_2-Ti_3Al layer was formed between δ-TiN and Ti.

3. As more Al atoms diffused into the δ-TiN layer, τ_1-Ti_3AlN was formed at the grain boundaries of δ-TiN, together with the exsolution of N atoms. The orientation relationships of δ-TiN and τ_1-Ti_3AlN were identified as $[111]_{\tau_1\text{-}Ti_3AlN}//[111]_{\delta\text{-}TiN}$ and $(1\bar{1}0)_{\tau_1\text{-}Ti_3AlN}//(1\bar{1}0)_{\delta\text{-}TiN}$.

4. The nitridization of the α_2-Ti_3Al layer due to the inward diffusion of the released N gave rise to the formation of δ-TiN and a twinned α_2-Ti_3Al(N) solid solution in the α_2-Ti_3Al layer upon annealing. The α_2-Ti_3Al(N) solid solution was transformed to the chopped fiber-like τ_1-Ti_3AlN structure during subsequent cooling. The orientation relationships of τ_1-Ti_3AlN and α_2-Ti_3Al in the twinned structure were as follows: $[111]_{\tau_1\text{-}Ti_3AlN}//[0001]_{\alpha_2\text{-}Ti_3Al}$ and $(0\bar{1}1)_{\tau_1\text{-}Ti_3AlN}//(\bar{1}\bar{1}20)_{\alpha_2\text{-}Ti_3Al}$.

5. Finally, the various stages of the interface reaction between AlN and Ti during annealing and cooling at 1000°C were proposed. The microstructural development of the AlN/Ti interface was related to the diffusion path in the isothermal section of the Al–N–Ti ternary phase diagram.

References

[1]X. He, K. Tao, and Y. Fan, "Solid-State Reaction of Ti and Ni Thin Film with Aluminum Nitride," *J. Vac. Sci. Technol.*, **14** [4] 2564–9 (1996).

[2]C. Tsai, J. Tseng, and C. His, "Interfacial Adhesion and Microstructure of Thick Film Metallized Aluminum Nitride Substrates," *Ceram. Int.*, **28**, 23–8 (2002).

[3]M. Borowski and J. P. Dallas, "Structural Characterization of Ti Implanted AlN," *J. Mater. Res.*, **12** [10] 3136–42 (1995).

[4]K. Komeya, "Development of Nitrogen Ceramics," *Am. Ceram. Soc. Bull.*, **63** [9] 1158–9 (1984).

[5]N. Kuramoto, H. Taniguchi, and I. Aso, "Translucent AlN Ceramic Substrate," *IEEE Trans. Compon. Hybrids Manuf. Technol.*, **CHMT-9** [4] 386–90 (1986).

[6]Y. Imanaka and M. R. Notis, "Interfacial Reaction Between Titanium Thin Films and Aluminum Nitride Substrates," *J. Am. Ceram. Soc.*, **82** [6] 1547–52 (1999).

[7]X. He, Si.-Ze. Yang, K. Tao, and Y. Fan, "Investigation of the Interface Reactions of Ti Thin Films with AlN Substrate," *J. Mater. Res.*, **12** [3] 846–51 (1997).

[8]M. Pinkas, N. Frage, N. Froumin, J. Pelleg, and M. P. Dariel, "Early Stages of Interface Reactions Between AlN and Ti Thin Films," *J. Vac. Sci. Technol.*, **20** [3] 887–96 (2002).

[9]T. Yasumoto, K. Amakawa, N. Iwase, and N. Shinsawa, "Reaction Between AlN and Metal Thin Films During High Temperature Annealing," *J. Ceram. Soc. Jpn.*, **101** [9] 969–73 (1993).

[10]R. Yue, Y. Wang, C. Chen, and C. Xu, "Interface Reaction of Ti and Mullite Ceramic Substrate," *Appl. Surf. Sci.*, **126**, 255–64 (1998).

[11]M. H. El-Sayed, M. Naka, and J. C. Schuster, "Interfacial Structure and Reaction Mechanism of AlN/Ti Joints," *J. Mater. Sci.*, **32**, 2715–21 (1997).

[12]Y. S. Han, K. B. Kalmykov, S. F. Dunaev, and A. I. Zaitsev, "Phase Equilibria in the Ti–Al–N System at 1273K," *Dok. Phys. Chem.*, **396** [2] 134–7 (2004).

[13]Y. Paransky, A. Berner, and I. Gotman, "Microstructure of Reaction Zone at the Ti–AlN Interface," *Mater. Lett.*, **40**, 180–6 (1999).

[14]Y. M. Paransky, A. I. Berner, I. Y. Gotman, and E. Y. Gutmanas, "Phase Recognition in AlN–Ti System by Energy Dispersive Spectroscopy and Electron Backscatter Diffraction," *Mikrochim. Acta*, **134**, 171–7 (2000).

[15]Y. Paransky, I. Gotman, and E. Y. Gutmanas, "Reactive Phase Formation at AlN–Ti and AlN–TiAl Interfaces," *Mater. Sci. Eng.*, **A277**, 83–94 (2000).

[16]C. H. Chiu and C. C. Lin, "Microstructural Characterization and Phase Development at the Interface Between Aluminum Nitride and Titanium After Annealing at 1300°–1500°C," *J. Am. Ceram. Soc.*, **89** [4] 1409–18 (2006).

[17]L. Hultman, "Thermal Stability of Nitride Thin Films," *Vacuum*, **57**, 1–30 (2000).

[18]J. C. Schuster and J. Bauer, "The Ternary System Titanium–Aluminum–Nitrogen," *J. Solid State Chem.*, **53** [2] 260–5 (1984).

[19]R. Yue, Y. Wang, Y. Wang, and C. Chen, "Study on Interfacial Reaction of Ti/AlN by SIMS, RBS and XRD," *Surf. Interface Anal.*, **27**, 98–102 (1999).

[20]J. Magnan, G. C. Weatherly, and M. C. Cheynet, "The Nitriding Behavior of Ti–Al Alloys at 1000°C," *Metall. Mater. Trans. A*, **30A**, 19–29 (1999).

[21]J. L. Murray, *Phase Diagrams of Binary Titanium Alloys*. ASM International, Metals Part, Ohio, 1987.

[22]H. Z. Xiao, I. M. Robertson, and H. K. Birnbaum, "Effects of Hydrogen on the Microstructure and Microchemistry of Ti_3Al-Nb Intermetallic at High Temperatures and High Pressures," *J. Mater. Res.*, **11** [9] 2186 (1996).

[23]P. Villars, A. Prince, and H. Okamoto, *Handbook of Ternary Alloy Phase Diagrams*. ASM International, Materials Part, Ohio, 1994. □